

INKJET PRINT QUALITY: THE ROLE OF POLYVINYL ALCOHOL IN SPECIALITY CaCO₃ COATINGS

T.Lamminmäki, J. P. Kettle, P. Puukko¹,
C. Ridgway³, P.A.C Gane²

¹T.Lamminmäki (taina.lamminmaki@kcl.fi), J.Kettle (john.kettle@kcl.fi), P.Puukko (pasi.puukko@kcl.fi): Oy Keskuslaboratorio, Tekniikantie 2, FIN-02150 Espoo, FINLAND,

² P.A.C.Gane (patrick.gane@tkk.fi and patrick.gane@omya.com), TKK, Vuorimiehentie 2, FIN-01250 Espoo, FINLAND, or OMYA Development AG, CH-4665 Oftringen, Switzerland,

³ C.Ridgway (cathy.ridgway@omya.com) OMYA Development AG, CH-4665 Oftringen, Switzerland

1 ABSTRACT

The aim of this work is to clarify the controlling role of polyvinyl alcohol (PVOH) as a binder in the formation of coating and pore structure and how it affects the high-speed inkjet image quality formation. The results show that the pigment type and the binder amount have a large interactive effect on pore structure formation. The optical properties of the whole paper, not just the coating, are the most important regarding print density, but the properties of the coating layer itself have a dominant effect when considering the ink bleeding.

2 BACKGROUND

There is an increasing trend for the use of aqueous-based inkjet inks in high-speed commercial printing, and this challenges the hydrophilic and absorptive properties of the surface of paper /1/. There is an urgent need to develop the coating layer properties based on the mechanisms which control these properties in inkjet printing, and the interaction of pigment and typical inkjet paper coating formulation binders, in determining coating pore structure, is an area that has received insufficient attention in this respect.

The absorption speed and volume of the ink diluent/solvent challenge the capacity of the paper surface to generate acceptable inkjet print quality. The water-solvent should absorb very rapidly into the paper so that different colours of inks do mix together in certain extent on the surface or intermingle in the structure of the sheet. Ink droplet setting is a phenomenon that happens on a millisecond scale, but the final ink drying can take hours /2/. The amount of applied solvent can be very high, so the paper needs a high porosity to get all of the water-solvent into the paper structure. Even in emerging systems where the volume of diluent is strictly controlled, the rate of absorption still plays a decisive role.

The absorption volume and speed is commonly explained adopting the Lucas-Washburn equation. According to Lucas-Washburn's equilibrium equation, the volume of liquid in a capillary should be greater, the larger the radius, at a given time. On the other hand, the practical studies have shown that smaller radius capillaries initially fill faster than larger

capillaries. Ink sets faster on a fine pore structure coating layer than on a highly porous, large pore containing coated paper. This disagrees with the model of Lucas-Washburn. Clearly, there is a distinction between fine and large pores, and, furthermore, there are effects occurring on the short timescale on the surface and in the pore network as well as in a single and several interconnected capillaries that Lucas-Washburn does not capture /3, 4, 5/.

Ridgway *et al.* /3/ studied further the Lucas-Washburn equation. They showed that there are a number of more detailed descriptions of flow entry effects into capillaries, such as the energy loss equation of Szekely /5/. Bosanquet /6/ added the inertial wetting term associated with an accelerating fluid. A solution of the equation of Bosanquet for short times is proposed by Schoelkopf *et al.* /7/, which showed that liquid penetration distance by absorption into the finest capillaries over short timescales has a direct proportionality to the time elapsed. When inertia dominates, the finest pores will absorb further and faster. Furthermore, if we consider a network of such fine pores, remembering that a fine pore in coatings is, typically, equally as short as its diameter is wide, then, in combination with enough reservoir volume between them, we can visualise a preferred pathway effectively by-passing the larger pores or at least limiting the access to them. This has been constructed by Ridgway *et al.* /8/ using the Pore-Cor¹ visualisation. In this pathway, the velocity of absorption is high, and so the passage into the porous medium is defined by the combination of pore sizes within the inertial wetting regime (nanopores) and the connecting reservoir structure consisting of larger pores which fill more slowly. So we can assume that small pores are needed for quick inkjet ink penetration at the moment of droplet setting and large pores are needed for the storage of all the solvents into the structure. The connectivity relation between these is crucial if the maximum absorption rate for large volumes is to be maintained.

In coating colours, we have, besides the pigments with their particle packing characteristics and internal pore structure, if present, the binder. By changing binder amount or binder type we can influence the inkjet ink penetration. First of all, the binder amount should be sufficient that the coating colour has an adequate adhesion to the paper surface and cohesion such that dusting problems are minimal. The surface strength is not needed at such high levels as in traditional offset printing, but nonetheless dust generation is critical, as it could lead to blockage or damage of the inkjet nozzles, and so diminish the print quality and reduce the lifetime of expensive print engine components. In coating colours for inkjet papers, polyvinyl alcohol (PVOH) is a very commonly used binder, and it has a high capability to bind pigments. It is also a very hydrophilic binder, and exhibits swelling on contact with water /9, 10, 11/. Pinto *et al.* /11/ showed in their study that ink diffusion is unrestrained by PVOH, and the colorant

¹ Pore-Cor and Pore-Comp are a software network model and sample compression correction software, respectively, developed by the Environmental and Fluid Modelling Group, University of Plymouth, PL4 8AA, UK.

concentration profile is uniform in a PVOH layer as shown by time-of-flight secondary ion mass spectrometry (TOF-SIMS) analysis. Lately, the binder type has been shown to have an effect on the inkjet ink print density and bleeding development, Nilsson /12/ and Svanholm /13/. However, the binder swelling tendency in inkjet print quality formation has not been studied so widely.

The aim of this work is to clarify

- the role of PVOH as a swelling binder in the porous CaCO₃ coating layer structure,
- the role of porosity and pore diameters in the inkjet ink setting process, and
- how the PVOH coatings work in the print quality formation of dye-based inks in high-speed inkjet printing.

3 MATERIALS AND METHODS

3.1 Coating compositions and coating trials

A range of calcium carbonate-based pigments provided by Omya AG² were used. One CaCO₃ pigment from Minerals Technology Europe³ was also included. The main variables of the pigments were mean particle diameter and specific surface area (Table 1). The binder was PVOH (Mowiol 40-88 provided by Clariant International AG⁴, which had a degree of hydrolysis 87.7 ± 1.0 %, and a molecular weight of 204 000 g mol⁻¹/14/).

The study was started by looking at the properties of pure pigments. Pigment cakes and 100 g m⁻² coating layers on glass plates were produced from a range of formulations. The cakes were made with Teflon moulds, drying them at 23°C temperature. The glass plates were coated with an Erichsen⁵ film applicator (Model 288) using blades with a fixed gap height between 100 and 500 µm. All the pigments had been dispersed by the pigment manufacturers themselves

The pigment properties are shown in Table 1. The choice of pigments was made to illustrate the effects of particle size and internal pore structure, including raw material sources from ground calcium carbonate (GCC), subsequently modified to generate high surface area and internal pores (MCC), and precipitated calcium carbonate (PCC). The pigment diameters were determined by sedimentation (Sedigraph 1500, Micromeritics⁶) or by laser light scattering (NanoSight⁷) and the values given are quoted from the specifications of the manufacturers. The pH and zeta-potential

(AcoustoSizer II⁸) were determined in the coating colour, which in this case contained 10 pph PVOH (based on 100 pph by weight pigment). We note that all but one of the pigments exhibit a cationic slurry property, being designed to adsorb anionic ink dye so as to prevent strike through and to maximise print density by concentrating the colorant near the coating surface. Coulombic interaction also acts to maintain water fastness of the ink.

The liquid uptake capacity of the porous structures was measured with Si-oil absorption. During the oil absorption, the pigment cake was left for one hour in Si-oil, and the weight of cake before and after Si-oil saturation was measured. The available porosity for oil absorption is defined as absorbed Si-oil volume in coating cake divided by the sum of the coating layer volume without oil plus absorbed Si-oil volume, all determined at normal air pressure.

The pore volume and pore size distribution was measured with mercury porosimetry (Micromeritics AutoPore IV⁵), adopting using the Pore-Comp¹ correction to account for penetrometer expansion, mercury compression and compression of the sample skeletal material, expressed as the elastic bulk modulus, according to Gane *et al.* /15/. The coatings with different binder amount were analysed up to 140 Pa (low pressure port) and 440 Pa (high pressure port), respectively. The coated glass plates were analysed by the thin layer chromatography method (TLC), putting the plate into the eluent (equivalent to the ink diluent alone). The distance of eluent movement during time was measured. The optical properties of the coating layer were studied as a function of eluent uptake and distance, e.g. opacity according to ISO 2471:98. Behind the coated glass plate a stock of blotting boards (fully bleached) was used as backing.

The KCL pilot coater was used to apply coatings on a larger scale to traditional base paper, which was chosen to be a commercial base sheet for a coated fine paper, 53 g m⁻². The base paper was first pre-coated so that the top coating of main interest was prevented from penetrating into the base paper. The pre-coating of 7 g m⁻² was applied with a film coater on both sides of the paper, and the actual studied coating layer of 8 g m⁻² with short dwell application (blade). The pre-coating had 100 pph of GCC (Hydrocarb 60), 12 pph styrene-butadiene latex and 0.6 pph carboxymethylcellulose. The recipes of the top coating are introduced in Table 2. The coating speed was 1 800 m min⁻¹ and the final moisture content of the coated web was 5 wt%.

² Omya AG, Postfach 32, CH-4665 Oftringen, Switzerland

³ Minerals Technologies Europe, Ikaros Business Park, Ikaroslaan 17, Box 27, 1930 Zaventem

⁴ Clariant International AG, Rothausstrasse 61, CH-4132 Muttenz 1, Switzerland

⁵ Erichsen GmbH & Co., Am Iserbach 14, D-58675 Hemer, Germany

⁶ Micromeritics Instrument Corporation, 4536 Communications Drive, Norcross, GA 30093, USA.

⁷ NanoSight Ltd., Minton Park, London Road, Amesbury, Wiltshire SP4 7RT, UK.

⁸ AcoustoSizer II is a product name of Colloidal Dynamics/Agilent, Technologies (Finland Oy), Linnoitustie 2B, FI-02600, Espoo, Finland

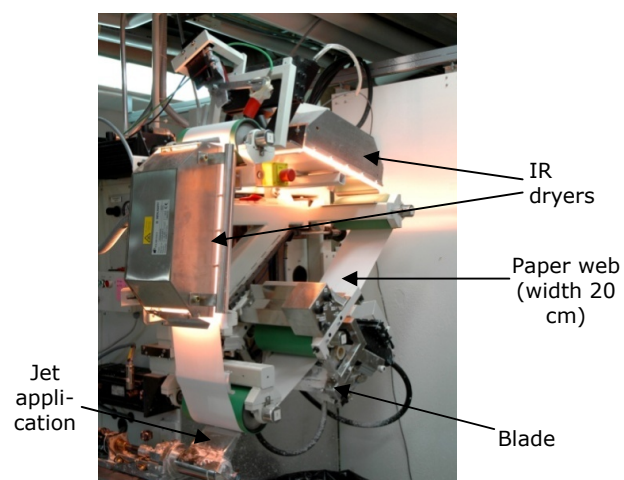
TABLE 1. PIGMENT PROPERTIES*) NanoSight (results had two peaks: small at 20-30 nm and average at 0.25 μm)

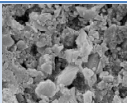
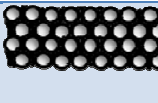
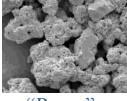
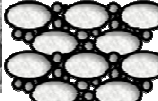



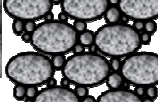
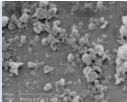

Properties	Ground calcium carbonate - GCC	Modified calcium carbonate - "MCC large"	Modified calcium carbonate - "MCC small"	Precipitated calcium carbonate - "PCC large"	Precipitated calcium carbonate - "PCC small"
Weight median pigment particle diameter, μm ($d_{50\%}$)	0.65	2.70	1.30	2.70	Small 0.02-0.03 Ave. 0.25 *)
Specific surface area, m^2g^{-1} (BET, ISO 9277)	10.7	46.2	27.0	63.7	73.9
Zeta-potential, mV (AcoustoSizer II)	-9	13.1	13.6	1.6	-0.6
Registered trade name	HYDROCARB 90	OMYAJET B6606	OMYA JET C3301	OMYA JET B5260	JetCoat 30

TABLE 2. THE TOP COATING COLOURS.

Pigment/ Binder	Colour 1	Colour 2	Colour 3	Colour 4
"PCC large"	100	100	100	
"PCC small"				100
PVOH	7	12	30	7

The role of pigment properties alone in the inkjet ink setting process was also studied, so as to identify subsequently the interactive roles of pigment and binder combined. In this case the coating was applied with a semi-pilot coater, KCL SAUKKO (Fig. 1), using jet application and blade. The coating was dried with two infra red dryers. The speed of the web was 900 m min^{-1} . The same base paper was used as in the pilot coating. Based on the pilot-trials the binder amount was selected to be 10 pph of PVOH (Mowiol 40-88) to represent commercially acceptable strength and anti-dusting properties. The structural illustrations of produced coatings are given in Table 3. The target coating layer amount of 10 gm^{-2} was not achieved in one single coating layer. The low solids content and the low viscosity of the coating colours limited the applied coating layer thickness, and therefore we had to apply the same coating colour twice.

**Fig. 1. Image of KCL SAUKKO /16/.****TABLE 3. THE STRUCTURAL ILLUSTRATION OF COATING LAYERS AFTER THE SAUKKO COATING. ALL COATINGS HAD 10 PPH PVOH.**

Pigment	Air permeance, $\mu\text{m}^3 (\text{Pa}\cdot\text{s})^{-1}$	Porosity (coating cakes), %	Structure of pigment	Illustrated coating layer structure
GCC	0.1	17.7	 Rhombohedral	
"MCC large"	1.3	46.2	 "Roses"	
"MCC small"	0.7	31.9	 "Roses"	
"PCC large"	1.8	48.9	 "Eggs"	
"PCC small"	2.3	32.9	 Spherical	

The air permeance of coated papers was measured with Parker-Print Surf measurement using pressure 20 kPa. The opacity was measured according to the standard ISO2471:98 and light scattering coefficient ISO 9416:98. The surface strength of coated papers was studied with an IGT device using ISO 3783:06 method with a medium viscosity oil. The absorption time of dye was measured with KCL DIGAT that has been introduced and described in detail in reference /17/. The ink was anionic dye-based ink (from a Versamark VX5000e) and applied ink amount was 8 gm^{-2} . The surface structure of the coating layer was imaged with the scanning electronic microscope (SEM).

3.2 Inkjet printed surfaces

Inkjet printing was carried out on a Versamark VX5000e, which produces inkjet droplets by the continuous stream inkjet method. The inks were dye-base and the main diluent/solvent was water. The surface tensions of the inks were observed to fall in the small range of 51-55 mN·m⁻¹ (25°C), depending on dye colour, and the viscosity was 1-2 mPa·s. Printing speed was 100 m·min⁻¹ and the drying drum and hot air dryer were set to a temperature of 80°C (when studying pigment type to emphasise absorption criteria) and 100°C (when studying the range of binder amount).

The print density of the printed surface was measured with GretagMacbeth D196. Both a camera and scanner systems were utilised to analyse the bleeding, in terms of distance from the formal colour boundary. The parallel reporting from the two systems was also a part of the development of the scanner method. In the camera system, a picture was taken with an imaging camera from a solid printed line used to define the bleeding boundary, and a grey level profile across the line was constructed. The normal edge width for the given print was measured as the distance between two points A and B. Point A was defined as the point at which the surface across the line image was 10 % brighter than the darkest region in the line, and B 10 % darker than a given background (unprinted area). The black surface had grey value zero and white 254. Each unprinted paper was adjusted to the value 170. The normal edge width described the bleeding distance of inks. The smaller the number, the sharper is the printed line. In the scanner system, an Epson Perfection V700 Photo was used, with a resolution of 2 400 dpi. The grey level profile of the line was again measured with an image analysis program using a similar definition of the points A and B, but now A was 15 % brighter than the darkest region and B 15 % darker than a background (unprinted area). The grey levels were adjusted as in the previous camera system. The differences in the optics caused some differences in the results between these methods.

The ink colorant penetration was studied by embedding the printed surface in LR White resin⁹. The embedded sample was placed in a refrigerator to reduce smearing of the dye. The cross-sections were then imaged in a light microscope (Zeiss Axioscope 2 plus).

4 RESULTS

4.1 PVOH and porosity formation of the coating layer

The intrinsic structure of the coating layer, without the influence of the base paper, was studied using the coating cake material. At this point, we have to remember that the structure of the coating cake, formed by drying a relatively large volume of coating colour, could be expected to be somewhat different to that of the structure of a thinly applied coating layer on a paper surface, where the coating process variables affect the forming structure, including differences in shrinkage behaviour. This issue has been resolved to some extent by the development of a pigment tablet formation device at Omya

AG /7/, however this was not used in this work as the PVOH binder is soluble, and filtration might have led to an unwanted depletion of binder. In this current work, however, we saw that the differences were in fact minimal between the measurements on the coated papers and the coating cakes.

The absorption capacity of the coating cakes was analysed with Si-oil absorption (Fig. 2). As expected, increasing the binder amount reduced the level of porosity as measured by this technique. At the binder level 10 pph, the porosities of fine particulate "MCC small" and "PCC small" pigments were found to be on the same level. The highest porosities were produced by the large particle size coatings. This illustrates the likely particle packing characteristics.

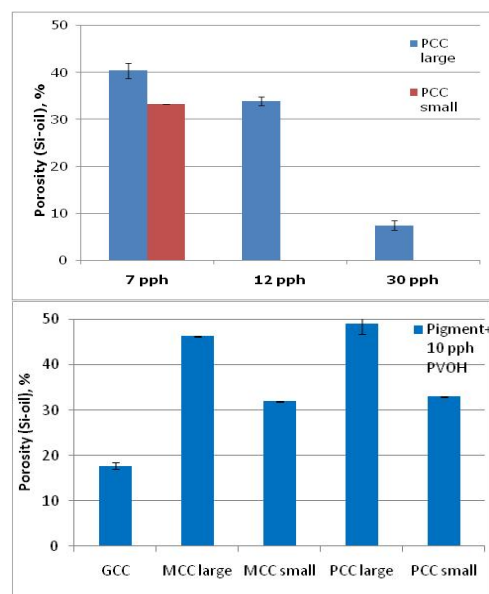


Fig. 2. Absorption capacity of pigment cakes as a function of PVOH binder level, measured by the Si-oil absorption method.

The porosities of the coating layers were also calculated from mercury porosimetry results, when the base paper effect and the amount of coating layer are taken account, following the method of Ridgway *et al.* /18/. The cumulative intruded pore volumes of the coating layers are illustrated in Fig. 3. The "PCC large" coating produced again the greatest pore volume, and it had more large size pores. The lowest porosities were seen for GCC and "MCC small".

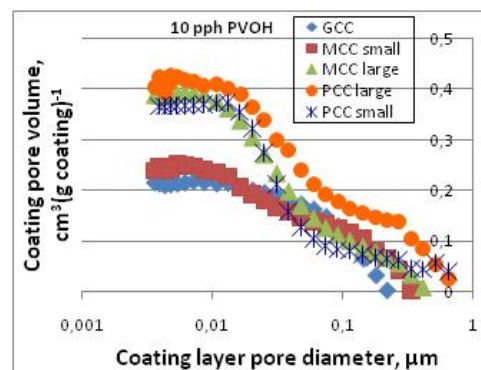


Fig. 3. The cumulative pore volume distributed as a function of pore size, as measured using mercury porosimetry.

⁹ Electron Microscopy Sciences, P.O. Box 550, 1560 Industry Road, Hatfield, PA-19440, USA

The results of Si-oil porosity and mercury porosimeter measurements correlate very well (Fig. 4). The slight differences can be analysed in respect to the high pressures used in the mercury measurement. At the final stages of mercury intrusion, the pressures are sufficiently high to compress any elastic components present as part of the skeletal structure of the porous material. Polymers, in particular binder, undergo such compressive effects. The result is an absence of hysteresis between the intrusion and extrusion curves as a function of pressure increase and decrease, respectively. The gradient of this elastic region can be determined and related to a bulk modulus expressing the volume compressibility of the material, Gane *et al.* /15/. The bulk modulus of the paper coating based on "PCC large" with 10 pph PVOH was $30.6 \cdot 10^3$ MPa and that containing "PCC small", also with 10 pph PVOH, was $22.0 \cdot 10^3$ MPa. This means that the large size pigment coating can resist pressure on the skeletal components more than "PCC small" paper. This reflects the distribution of polymer in respect to the pigment particle packing and the pore sizes present. The finer pigment, with its higher surface area, will necessarily present more polymer species and amount, including dispersant, to the coating colour.

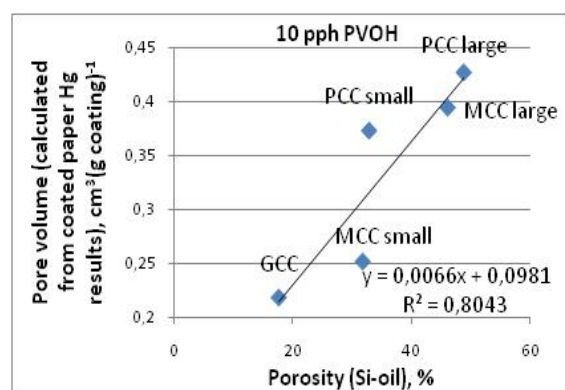


Fig. 4. Correlation between the results of Si-oil porosity and mercury porosimeter.

The pigment *cakes* made from "MCC small" and "PCC small" with binder had very similar Si-oil absorption volume capacities, as seen in Fig. 4, but exhibited very different porosity when analysed with the mercury porosimeter. This lets us deduce, that binder tends to blank off the entry to, or connectivity between, pores. Thus, the oil cannot access all the pore volume, whereas the intruding mercury can break through the pore-blanking binder films. This effect is confirmed by the equivalence between the two methods for the pigment cakes without PVOH, in which both techniques access the same pore volumes.

Traditionally, taking the first derivative of the cumulative mercury intrusion curves provides a pore size distribution. This description, although limited to an equivalent bundle of capillaries, and thus ignoring pore shielding effects, is nonetheless useful for comparison purposes between topologically similar structures Gane *et al.* /19/. We see that the PCC coating structure has only ultrafine pores in the 20-60 nm range. In contrast, the MCC coatings have both large and small-size pores, indicating that the MCC structures have both

intra- and inter-particle pores (Fig. 5). The addition of 10 pph PVOH decreases the pore volume of the MCC coating structure more than that of PCC. The peak of intra-particle pores of the MCC pigment decreases most markedly, clearly indicating that PVOH has filled intra-particle pores.

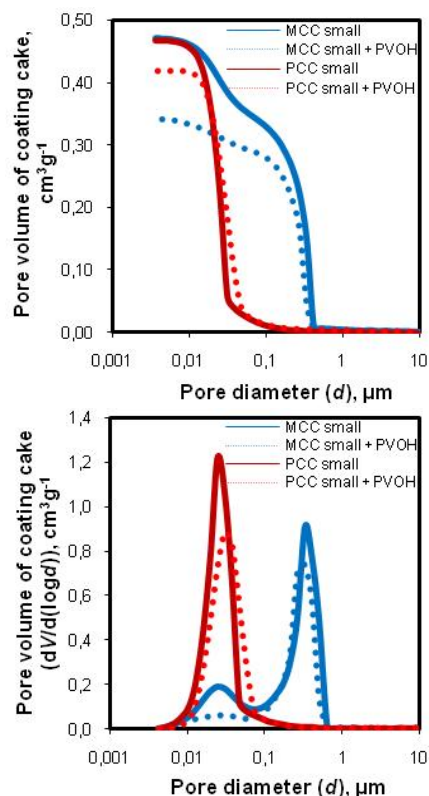


Fig. 5. Cumulative pore volume and pore size distribution curves of "MCC small" and "PCC small".

4.2 Effect of pigment properties on internal liquid transport

The thin layer chromatography method was used to analyse the eluent movement through the pore networks of the pure pigment packing structures. Long time passage of liquid through a porous network is defined by the surface wetting force resisted inversely by the permeability of the structure. The greater the permeability and the more the occurrence of fine pore structure surrounding that permeable pathway, the greater will be the transport length in a given time. The longest water/ethanol eluent transport distance through the structure was achieved with the most porous pigments (Fig. 6). The "MCC large" and "PCC large" pigments have very similar size and amount of intra-pigment pores, but MCC has smaller inter-particle pores and so less large pores to contribute to permeability, as Fig. 11 later shows. The GCC and "MCC small" coatings have quite similar capability to transport eluent. The distances are short because of the lack of permeability. The "PCC small" pigment unexpectedly transfers the liquid further in the structure than the other pigments. This would not be expected when looking purely at the fine pore structure, but the sample structures made from the "PCC small" pigment had a multitude of cracks, which contribute to the permeable transfer of eluent effectively in the pigment layer. This effect is not one of intrinsic particle

packing, but the response to shrinkage as the layer forms. These cracks are seen as essential if this pigment is to work in transporting liquid. The results indicate that pigments with higher pore volume transfer liquid more effectively than the lower pore volume structures depending on permeability.

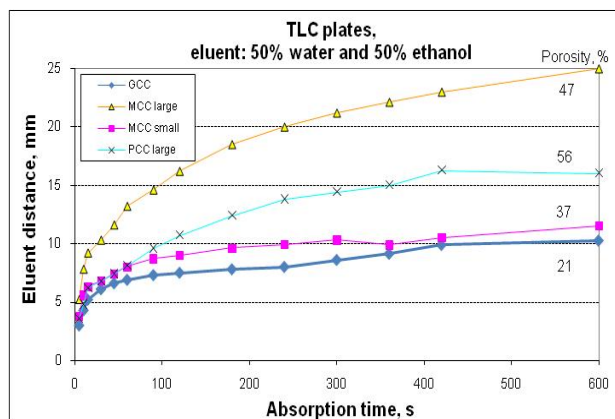


Fig. 6. Water/ethanol eluent transfer over time in the thin layer pigment chromatography layers formed on glass plates without binder.

4.3 Coating layer structure on paper surface

4.3.1 Role of binder

The higher binder amount increased the surface strength of coated papers (Fig. 7). The “PCC small” produced a little higher picking resistance with 7 pph binder amount than “PCC large”. Once again, this is due to the difference in interior structure permeability determining the level of binder depletion likely to occur when applied to an absorbent substrate. The surface strength of 2 ms^{-1} , defined as the speed at which the tack oil begins to induce pick from the coated paper in the test nip, is considered high enough to ensure attachment of the coating to the paper substrate and to prevent dusting during the inkjet printing.

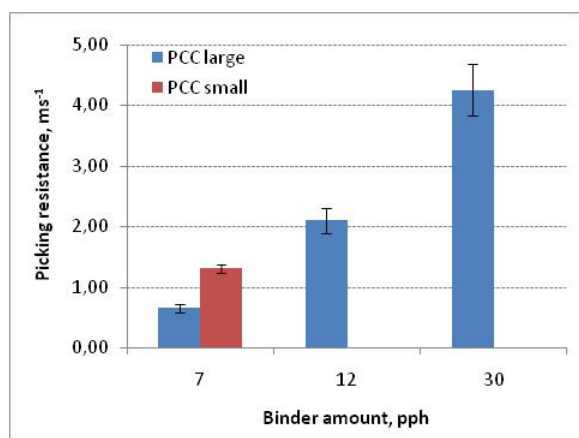


Fig. 7. Surface strength of coated papers measured with the IGT pick test method.

Fig. 8 shows how the binder amount increase decreases most of all the volume associated with the 30-50 nm size pores within the pore diameter area 0-0.1 μm , primarily responsible for the capillary driven absorption.

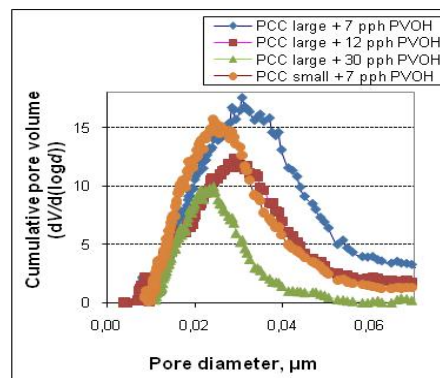


Fig. 8. The first derivative of the cumulative mercury intrusion curves (Pascal porosimeter).

The absorption speed into the thin layer coatings on glass using the DIGAT apparatus, therefore, became longer as the binder amount increased (Fig. 9). It was based on surface strength versus ink absorption speed results, that the PVOH amount of 10 pph was selected for our studies.

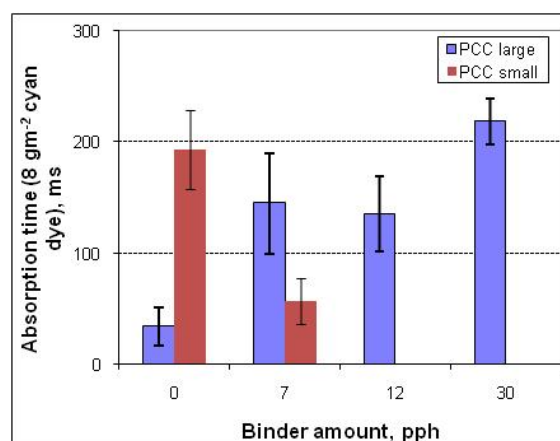


Fig. 9. Effect of binder amount on absorption time (DIGAT) for PCC coatings on glass plate.

The binder amount had very minimal effect on print density in the case of the “PCC large” structures. However, the pigment change from “PCC large” to “PCC small” clearly increased the print density. The binder, therefore, is unable at these levels to block the larger pores of the “PCC large” structure, which mostly determine the colorant transport.

Increase of the binder amount generated a significant increase in the amount of bleeding. The coatings with 12 pph and 30 pph of PVOH produced the widest bleeding distance (Fig. 9). Interestingly, the bleeding did not increase indefinitely as the binder amount increased, but rather plateaued, showing the loss of pore volume is likely to be countered by the swelling nature of the PVOH in its ability to absorb and hold liquid once sufficient PVOH is present.

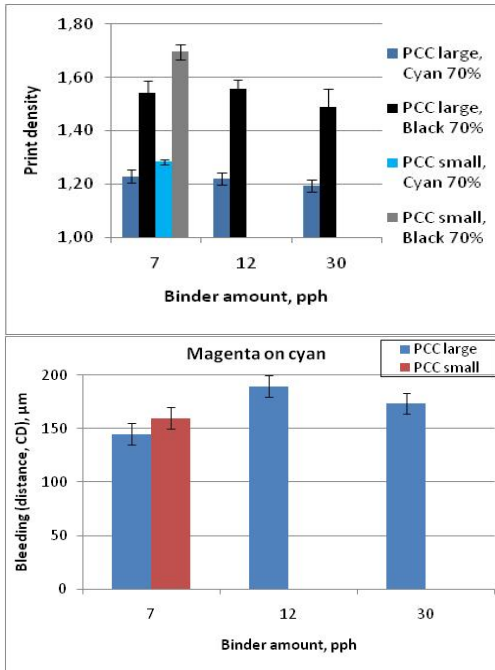


Fig. 9. Print density and bleeding distance of dye-based ink printed on PCC surfaces as a function of PVOH content.

4.3.2 Effect of pigment variables

Fig. 10 shows the cumulative pore volume intrusion by mercury of the coated papers which had been produced with five different pigments which were produced with double coating of same coating colour. The coating layers have partly penetrated into the base paper structure. All of the coated papers have lower pore volume results in the area of 1-10 μm than the base paper before coating.

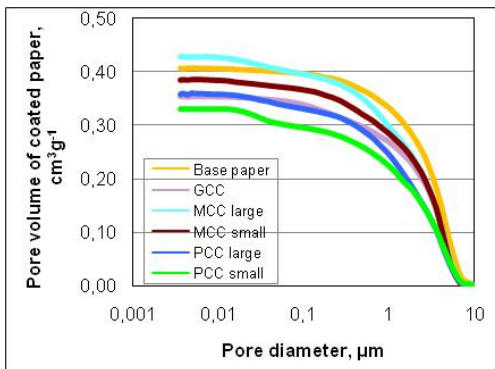


Fig. 10. The cumulative mercury intruded pore volume of coated papers. All coatings had 10 pph of PVOH.

The pore size distributions of the studied coatings are illustrated in Fig. 11. Generally, the pore size distributions of the coatings on paper reflected the main features of those of the cakes and of the thin layer chromatographic slides. "MCC large", "PCC large" and "PCC small" coatings have small pores, 20-40 nm in diameter, whereas GCC and "MCC small" had clearly less of such small pores. The coatings with the two large 2.7 μm diameter pigments ("MCC large" and "PCC large") had the same amount of small-scale pores. The GCC coating had mainly 0.1-0.3 μm diameter pores and "PCC large" had the largest diameter pores, 1.0-1.3 μm . "MCC

large" and "PCC large" had both small and large-scale pores. "PCC small" coating had mainly only small-scale pores.

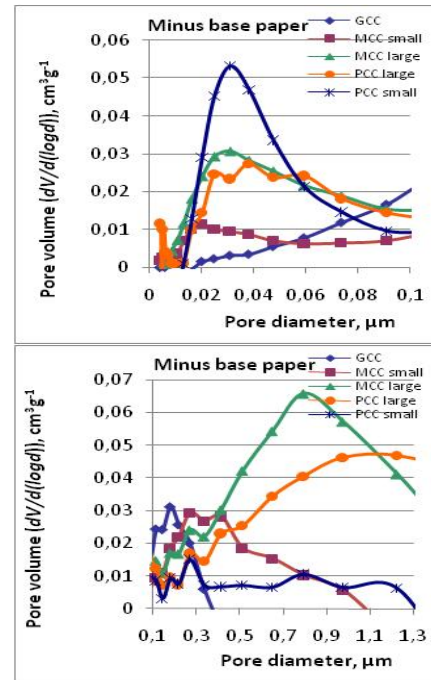


Fig. 11. The pore size distribution curves from mercury porosimetry of studied coated papers. The base paper values have subtracted from the results. The coatings have 10 pph PVOH.

The absorption speed into the coated papers was quickest with "PCC large". The slowest absorption was, as to be expected, with GCC (Fig. 12). The relative requirements of capillarity and permeability are well reflected in these data. The capillarity being provided by the ultrafine pores and the liquid transfer by the permeability of the coating layer, Ridgway and Gane /20/.

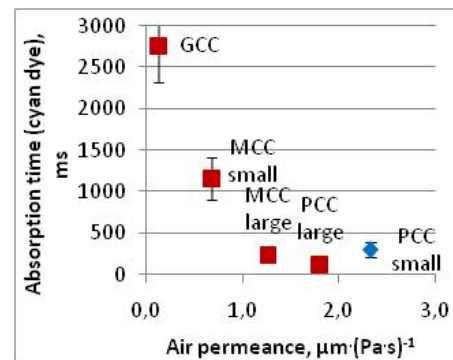


Fig. 12. Effect of air permeance on absorption speed (DIGAT).

The highest print density (Fig. 13) was achieved with the coating structure on paper derived from "PCC small", and the lowest from "MCC large". At the same time, "MCC large" and "PCC large" coatings produced the lowest bleeding values.

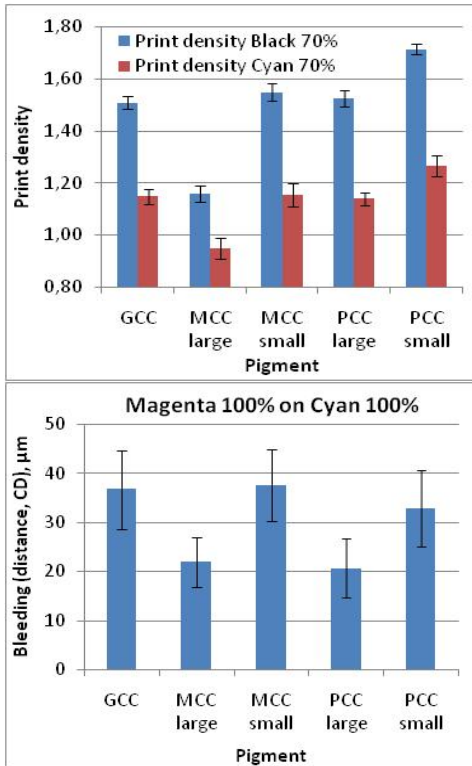


Fig. 13. Effect of coating pigment type on print density and bleeding (distance, measured with camera system) of dyes.

5 DISCUSSION

5.1 Role of PVOH swelling

We can assume, on the basis of mercury porosimetry results, that PVOH binder can go into or cap (film over the entry) intra- as well as the connecting pores, and exists around the larger inter-particle pores. At sufficiently high levels, any interaction of the binder with the liquid phase of the ink becomes important, not only in the structural modification of pore volume but in the diffusion of liquid through the polymer network, effecting swelling in the case of PVOH.

If we consider the binder layer thickness that might be present on the pigment surface, assuming to a first approximation a homogeneous distribution, it will depend on the specific surface area of pigment (thicker binder film at lower specific surface). The geometry of the pore is also assumed to be simple, such that the binder forms a uniform layer on the interior surface of the circular equivalent capillary, thus controlling the capillary diameter. In this way, we can calculate how the pore entrance area changes during the binder swelling process.

PVOH is a hydrophilic binder [10, 11]. Fig. 14 illustrates how a PVOH film (200-250 μm) absorbs water but not non-polar hexane. The PVOH film exhibited a 30.2 % swelling when exposed to cyan dye-based ink (Versamark VX5000e) after 30 s, and this value has been used in our calculations.

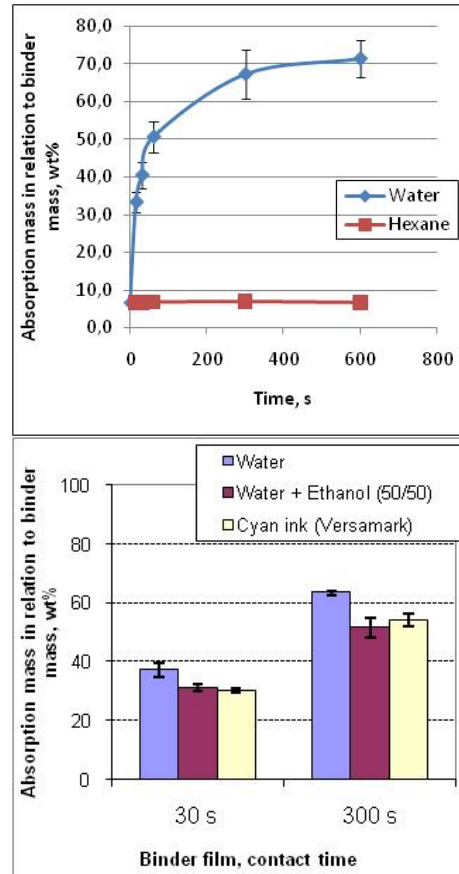


Fig. 14. Absorption amount of PVOH films. Assumed a specific gravity of water = 1 and that of PVOH = 1.26 then ratio the swelling fraction is given by (mass of water absorbed/mass of binder)*100.

The results of the calculation are illustrated in Fig. 15. The pore volume and amount of binder represents that to be found in 1 g of coating structure, as taken from mercury porosimetry and the coating formulation, respectively. The blue line is the pore area when the structure has been formed from pigments alone. The addition of 10 pph binder into the coating closes the below 10 nm diameter pores. The closing point of pore size, however, transfers to a diameter of 25 nm when a binder swelling of 30.2 % is taken account. The higher amount of binder increases the thickness of binder film and thus increases the effect of swelling. It seems that the swelling affects most or nearly all of the intra-particle pores. This means that these pores are effectively acting purely via a binder-swelling liquid uptake mechanism.

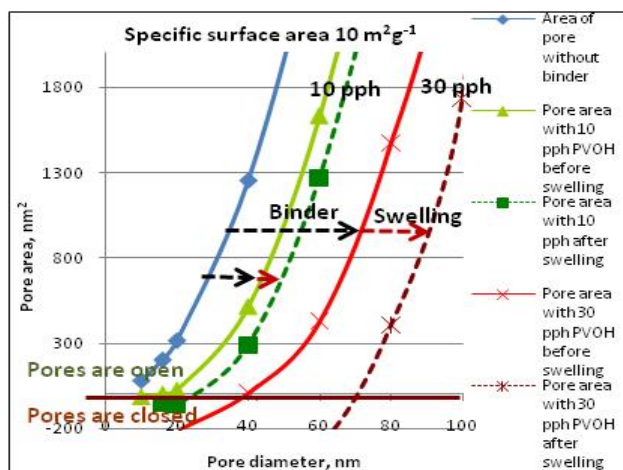


Fig. 15. The theoretical calculation of PVOH swelling effects. The coating amount was 1 g and density of PVOH 1.26 gcm^{-3} . The swelling of PVOH film was 30.2 % after 30 s (cyan dye).

So in theory, the binder swelling can affect the absorption speed of inkjet inks through the closing up of small pores. Table 4 shows the extent of the long time delays that exist in the inkjet printing machine. At 15 mmin^{-1} speed, the delay between the first inkjet nozzles to the beginning of drying is 17 s, and to the end of drying 25 s. The 30 s time considered in binder swelling is within this same timescale. The effect of swelling diminishes when liquid has less time to affect the binder, as Fig. 14 shows, and therefore we can assume that swelling has a smaller role at higher printing speeds, but it will not totally disappear. Thus, diffusion into polymer networks can occur within the timescale of inkjet printing, even at high speeds.

TABLE 4. TIME DELAYS IN THE VERSAMARK VX5000E PRINTING PRESS.

	Speed 15 mmin^{-1}	Speed 100 mmin^{-1}
Cyan to yellow (CMKY)	5 s	0.8 s
Yellow to drying beginning	12 s	1.8 s
Drying beginning to end	8 s	1.2 s
SUMMARY	25 s	3.8 s

5.2 How does PVOH work with different types of calcium carbonates?

From the optical point of view, "PCC small" pigment particles are so fine that they cannot scatter light effectively, and, in that sense, the pigment is optically inactive (Fig. 16). According to the theory of Kubelka-Munk /21/, those particles which have a diameter of the order of the wavelength of light ($0.1\text{-}1 \mu\text{m}$) affect strongly the light scattering. The opacity and light scattering coefficient of the "PCC small" coating layer remains lower because the pigment size is so small, 20-30 nm. The results agree with other previous results /22, 23/. The other pigments had quite similar opacities on glass plates.

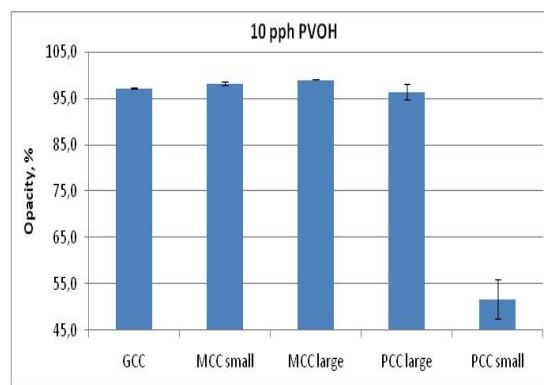


Fig. 16. Opacity of coating layers on the glass plate (100 gm^{-2}).

The optical properties of the *whole coated paper* dominate the print density formation. The "PCC small" is virtually optically inert (Fig. 17), whereas the other pigments affect the print density more. The correlation between the pore volume of the whole paper and print density was in the range $-0.904 - -0.949$, whereas correlation between the pore volume of the coating layer alone and print density was as low as $-0.050 - -0.217$. The whole paper structure, therefore, takes a part in the print density formation, not only the coating layer. This of course depends on the nature of the base paper, but if optically interactive it will contribute to the background light white noise and so reduce print density, especially of penetrated dye-based inks.

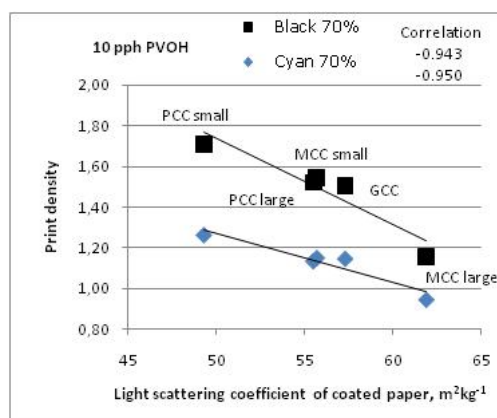


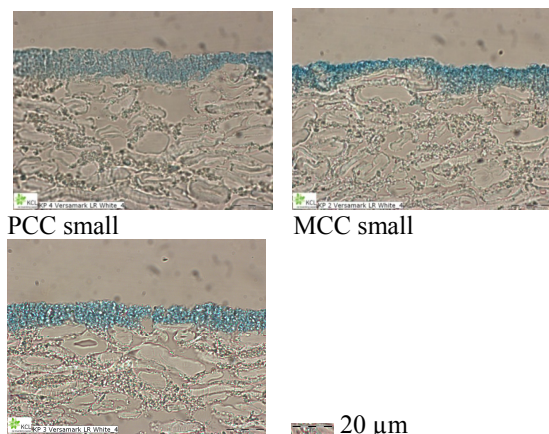
Fig. 17. Effect of light scattering coefficient on print density.

In these experiments, where speciality coating was applied to a pre-coated paper, the colorants stay in the coating layers and do not penetrate into the base paper (Fig. 18). However, it seems that the colorant is quite uniformly distributed in the coating layer including "MCC large". Even the cationic nature of the "MCC large" pigment did not fix the colorants in a manner that was visibly differently from the anionic pre-coat GCC. This suggests that either (i) the surface area is insufficient to trap all the colorant, (ii) the ink does not encounter the cationic nature of the pigment or (iii) the coating is too permeable to provide surface contact for all the colorant as it flows through the structure. There is some slight detectable concentration gradient for the finer MCC pigments, and this reflects the reduced internal pore network permeability.

TABLE 5. CORRELATIONS BETWEEN BLEEDING DISTANCES AND PORE STRUCTURE PROPERTIES.

Paper property	Bleeding distance		
	Magenta on cyan	Black on cyan	Black on yellow
Pore volume of coating layer	-0.898	-0.951	-0.943
Ink absorption speed (cyan)	0.653	0.745	0.994
Air permeance	-0.575	-0.786	-0.883
Surface energy of coated paper*	-0.653	-0.724	-0.978
Pore volume of whole paper	-0.210	0.063	-0.104

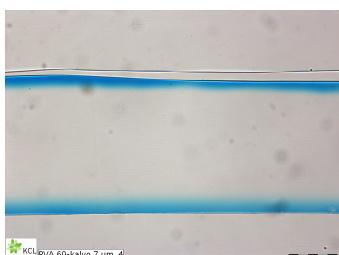
*Surface energy as defined by the sessile drop model, albeit a gross approximation for absorbent surfaces.



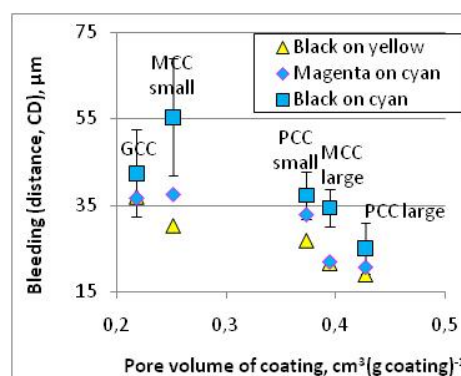
MCC large

Fig. 18. Cross-section dye-base ink printed surfaces.

The cross-section in Fig. 19 is of a PVOH film absorbed with cyan ink. It shows that ink colorants have penetrated into the binder film after 30 s absorption time, but not completely. The colorants, therefore, can be expected to diffuse into the PVOH layer together with the water. The result is in good agreement with the observations of Oka *et al.* /24/ and Svanholm *et al.* /25/. In a coating structure, colorants are distributed quite uniformly through the coating layer. This could be an indication that PVOH has covered the pigments and colorants are predominantly in the PVOH. Therefore, the pigment type or charge has very minimal effect on colorant location when PVOH is used as binder.

**Fig. 19. Cross-section figure of cyan dye-based ink into PVOH film after 30 s ink absorption.**

The bleeding distance (Fig. 20), however, seems to be dependent on the pore volume of the *coating layer*, but not the pore volume of the whole paper. This confirms the lack of transfer of ink to the base paper for these coating layer configurations. Table 5 shows all the porosity related aspects of coating layer correlate well with bleeding. In addition, the increase of surface energy decreases the bleeding distance.

**Fig. 20. Bleeding of the studied coated surfaces. Bleeding measured with high-resolution camera.**

The large porosity "MCC large" and "PCC large" coatings had quite similar amount and size of the fine pores, but in the large-size area of the bimodal distribution (inter-particle pores), the "PCC large" has about 1.2 µm diameter pores whereas the "MCC large" has smaller inter-particle pores at 0.8 µm. The larger pores of PCC allow ink to penetrate more quickly into the coating structure and the bleeding formed is, therefore, less. In addition, the binder swelling influences more strongly in the MCC pigment coating than in the PCC. The thickness of binder layer is higher on the MCC coating because the specific surface area of pigment is lower.

The PVOH swelling phenomenon should have a strong effect on GCC and "MCC small" coatings, which have less of the ultrafine 20-60 nm diameter pores than the other pigments. As the "MCC small" does have some more of the smaller pores than GCC, so the swelling should affect mostly these pores, rendering them ineffective. The bleeding values are indeed quite similar.

Comparing the "MCC small" and "PCC small" coatings, the porosities are quite similar, but "PCC small" has more of the finest pores. The "MCC small" coating absorbs ink clearly slower than "PCC small". The binder swelling closes up pores during the ink absorption process. It seems that in our medium porosity area, the coating with smaller pores give less bleeding. This illustrates that the bleeding effect is surface absorption rapidity defined.

5.3 Effect of binder amount

"PCC large" and "PCC small" pigments were studied more closely by using different PVOH amounts. All the print density results are very near each other (Fig. 21). The cross-section images from printed papers (Fig. 22) indicate that the colorants of ink distribute within the coating layer at 7 pph PVOH and at these coat weights do not penetrate into the base paper. At 30 pph PVOH in the coating, colorants are concentrated more in the top layer of the coating. However, there are places where the colorants have moved into the base paper due to insufficient accessible pore volume in the coating, and this decreases the print density. The results of light scattering (S -coefficient 52.9 - 54.1 m^2kg^{-1}) from all the papers are very near each other. So, knowing that the pigments have very different light scattering, the whole paper properties as well dominate in this respect.

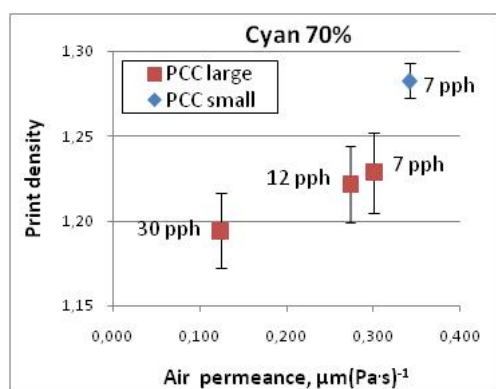


Fig. 21. Connections between print density and air permeance as a function of PVOH amount.

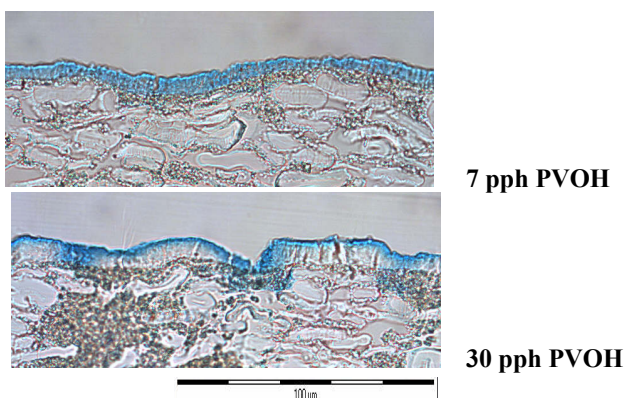


Fig. 22. Cross-section images of coatings containing different amounts of PVOH, that have been printed with cyan dyes.

Again, the bleeding distance depends on the fine pore coating properties. Therefore, not unsurprisingly, the least bleeding distance is reached with the lowest binder content coating (Fig. 23). The higher binder amount increases the bleeding.

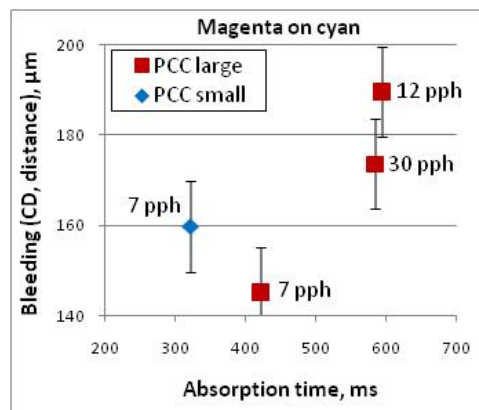


Fig. 23. Bleeding distance against absorption time. Measurement by scanner system and absorption time with DIGAT.

Fig. 24 shows that absorption time gets longer when binder amount increases from 7 pph to 12 pph. However, the 30 pph of binder is on the same level as 12 pph. These results are similar to those of Nilsson *et al.* /12/. When the binder amount is lower the ink moves into the coating layer mainly by capillary flow. At 30 pph binder amount, smaller capillaries are already closed and the dominating liquid transfer mechanism is diffusion in the binder layer, as Gane *et al.* /26/ indicate for their case of swelling polyacrylate dispersant covering the pigment surface. However, once a PVOH threshold amount is reached, specific for each pigment, this diffusion dominates and so provides a constant absorption speed from that binder level upwards (Fig. 24). The threshold point for the influence of binder swelling within these coatings should be expected at a binder amount of 12 pph.

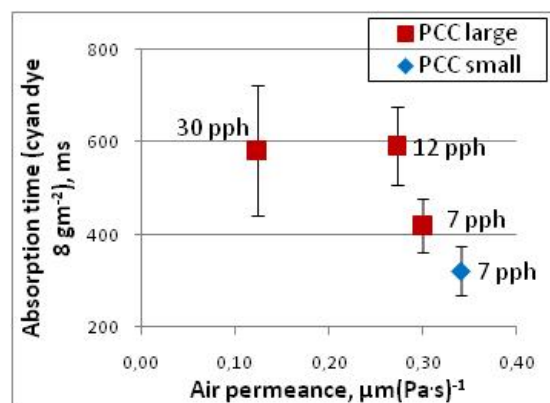


Fig. 24. Effect of PVOH amount in relation to air permeance and absorption time of cyan dye.

Another significant problem with the 30 pph coating is the coating layer distribution. The SEM image (Fig. 25) shows that the 30 pph PVOH coating layer is not very uniform and there are places where the binder has formed film-like layers which exhibit significant clumping together. As a result, distributed across the film-like layer there can also be seen holes.

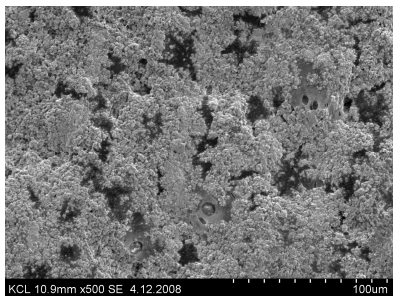


Fig. 25. Topographic image (SEM) of 30 pph PVOH "PCC large" pigment coating.

6 CONCLUSIONS

The major controlling parameters for liquid ink absorption into porous inkjet coating structures are confirmed to be *capillarity and permeability* in relation to the fine pores and the larger interconnected pores, respectively. A quick absorption of ink can be reached even with medium porosity coating structures, provided the coating has a lot of nano-size pores. In the case of porous pigment particles, such as modified or structured calcium carbonate, the fine pores are associated with intra-particle pores and the larger pores are defined by the particle packing.

The role of *PVOH binder* is shown to be complex in relation to pore structure modification and its affect on liquid uptake by diffusion. PVOH is shown to swell during the diffusion process. Although the volume of liquid imbibition related to PVOH swelling can be small at low binder levels, it acts to dominate the ink interaction with the pigment surface and the fine pore structure as binder levels increase, even at those levels required to prevent dusting. It seems that the colorants of dye-based inks locate more uniformly in the coating structure because PVOH covers the pigment surfaces and masks any surface cationicity of the pigment. The dye follows the aqueous liquid as it diffuses into the surface layer of PVOH. The impact of diffusion processes is even seen at high printing speeds, though the shorter the time to reach dryers, if present, the less is the volume of liquid involved. The swelling affects especially the accessibility to the intra-pigment pores of porous pigments.

The *coating layer* properties have a connection to print quality via the ink absorption speed and volume capacity. Too slow speed at the coating surface means that the colorants have more time to mix together and bleeding problems are more visible. The surface energy of the coating layer affects the colorant movement, too.

The optical properties of the *whole coated paper* dominate the print density achievable. This is because inkjet coating pigments are generally designed to have low scattering potential and so the base paper, if optically active, has a strong show through effect through the coating layer.

REFERENCES

1. SMYTH, S., "The Future of Inkjet Printing to 2013", PIRA International Ltd, 182 p. (2008).
2. SWERIN, A., KÖNIG, A., ANDERSSON, K., LINDGREN, E., "The use of silica pigments in coated media for inkjet printing: Effects of absorption and porosity on printing performance", 23. PTS Coating Symposium 2007, Baden-Baden, Germany, 18-20 September 2007, 15 p (2007).
3. RIDGWAY, C.J., GANE, P.A.C., SCHOELKOPF, J., "Effect of Capillary Element Aspect Ratio on the Dynamic Imbibition within Porous Networks", Journal of Colloid and Interface Science 252, 373-382 (2002).
4. SCHOELKOPF, J., GANE, P.A.C., RIDGWAY, C.J., MATTHEWS, G.P., "Practical observation of deviation from Lucas-Washburn scaling in porous media", Colloids and Surfaces A: Physicochemical and Engineering Aspects, 206 Issues 1-3, 445-454 (2002).
5. SORBIE, K.S., WU, Y.Z., MCDUGALL, S.R., "The Extended Washburn Equation and Its Application to the Oil/Water Pore Doublet Problem", Journal of Colloid and Interface Science 174, Issue 2, 289-301 (1995).
6. BOSANQUET, C. M., "On the flow of liquids into capillary tubes", Philosophical Magazine, Serie 6, 45(267): 525-531 (1923)
7. SCHOELKOPF, J., RIDGWAY, C.J., GANE, P.A.C., MATTHEWS, G.P., SPIELMANN, D.C., "Measurement and Network Modelling of Liquid Permeation into Compacted Mineral Blocks", Journal of Colloid and Interface Science 227(1), 119-131 (2000).
8. RIDGWAY, C.J., SCHOELKOPF, J., MATTHEWS, G.P., GANE, P.A.C., JAMES, P.W., "The Effects of Void Geometry and Contact Angle on the Absorption of Liquids into Porous Calcium Carbonate Structures", Journal of Colloid and Interface Science 239, 417-431 (2001).
9. CHAPMAN, D.M., "Coating structure effects on ink-jet print quality", TAPPI Coating Conference 1997, 11-14 May 1997, Philadelphia, Pennsylvania, USA, TAPPI, 73-93 (1997).
10. HARA, K., "Speciality PVOH in Ink Jet Coating Formulations", Paper Technology 47(3), 27-30 (2006).
11. PINTO, J., NICHOLAS M., "SIMS Studies of Ink Jet Media", IS&T's NIP 13: International Conference on Digital Printing Technologies, 2-7 November 1997, Seattle, Washington, 420-426 (1997).
12. NILSSON, H., FOGDEN, A., "Inkjet print quality on model paper coatings", Appita 61 (2), 120-127 (2008).
13. SVANHOLM, E., WEDIN, P., STRÖM, G., FOGDEN, A., "Colorant Migration in Mesoporous Inkjet Receptive Coatings", 9th TAPPI Advanced Coating Fundamentals Symposium, February 8-10 2006, Turku, Finland, 221-228 (2006).

14. Mowiol Polyvinyl Alcohol, procure of the chemical, Clariant, (1999).
15. GANE, P.A., KETTLE, J.P., MATTHEWS, G.P., RIDGWAY, C.J., "Void Space Structure of Compressible Polymer Spheres and Consolidated Calcium Carbonate Paper-Coating Formulations, *Ind.Eng.Chem.Res* 35(5), 1753-1764 (1996).
16. PAJARI, H., JUVONEN, K., JOKIO, M., KOSKELA, H., SNECK, A., "Dynamic measurement of coating colour consolidation with a new laboratory coater", 23rd PTS Coating Symposium, Baden-Baden, Germany, 18-21 Sept. 2007, Paper 28, 14pp.
17. LAMMINMÄKI, T., PUUKKO, P., "New ink absorption method to predict inkjet print quality", *Advances in Printing and Media Technology*, 34th International Research Conference of Iarigai, Grenoble, France, September 2007, 231-239 (2007).
18. RIDGWAY, C., GANE, P.A.C., "Bulk density measurement and coating porosity calculation for coated paper samples", *Nordic Pulp and Paper Research Journal* 18(1), 24-31 (2003).
19. GANE P.A.C., SALO M., KETTLE J.P., RIDGWAY C.J., "Comparison of Young-Laplace Pore Size and Microscopic Void Area Distributions in Topologically Similar Structures: a new method for characterising connectivity in pigmented coatings", *Journal of Materials Science*, (DOI: 10.1007/s10853-008-3134-8) *J Mater Sci* (2009) 44(2):422–432.
20. RIDGWAY C.J., GANE P.A.C., "Modified Calcium Carbonate Coatings with Rapid Absorption and Extensive Liquid Uptake Capacity", *Colloids and Surfaces, A: Physicochem. and Eng. Asp.*, 2004, vol 236/1-3 pp 91-102.
21. KUBELKA, P., MUNK, F., "Ein Beitrag zur Optik der Farbanstriche", *Z. techn. Physik* 12 (11a), 593-601 (1931).
22. DONIGIAN, D.W., "Ink jet dye fixation and coating pigments", *TAPPI Coating Conference* 1998, 4-6 May 1998, New Orleans, LA, USA, TAPPI, 393-412 (1998).
23. McFADDEN, M.G., DONIGIAN, D.W., "Effect of Coating Structure and Optics on Inkjet Printability", *TAPPI Coating Conference*, May 2-5 1999, Toronto, Canada, 169-177 (1999).
24. OKA, H., KIMURA, A., "The Physicochemical Environment of Acid red 249 Insolubilized in an Ink-Jet Paper", *Journal of Imaging Science and technology* 39(3), 239-243 (1995).
25. SVANHOLM, E., STRÖM, G., "Influence of polyvinyl alcohol on inkjet printability", *International Printing and Graphic Arts Conference*, Vancouver, BC, Canada, 4-6 October 2004, PAPTAC, 187-207 (2004).
26. GANE, P.A.C., RIDGWAY, C.J., "Moisture Pickup in Calcium Carbonate Coating Structures: role of surface and pore structure geometry", *Tappi 10th Advanced Coating Fundamentals Symposium*, June 11-13, 2008, Montreal, Canada, 24 p (2008).